

Enhancement of magnetoelectric effect in multiferroic fibrous nanocomposites via size-dependent material properties

E. Pan,^{1,a)} X. Wang,² and R. Wang¹

¹Computer Modeling and Simulation Group, College of Engineering, University of Akron, Akron, Ohio 44325-3905, USA

²Department of Mechanical Engineering and Center for Composite Materials, University of Delaware, Newark, Delaware 19716, USA

(Received 28 August 2009; accepted 12 October 2009; published online 2 November 2009)

We investigate the effective material properties of a multiferroic fibrous nanocomposite with size effects along its interface. The closed-form expression of the effective moduli of the nanocomposite shows that its response with interface effects depends on the size of the embedded fibers in the composite, a phenomenon different from the result based on the classical theory. We further demonstrate that the magnetoelectric effect can be substantially enhanced via proper design of the interface, providing an alternative avenue for controlling and, in particularly, increasing the magnetoelectric effect. © 2009 American Institute of Physics. [doi:10.1063/1.3257980]

The magnetoelectric (ME) effect in multiferroic composites, defined as the ratio between the magnetic (electric) field output over the electric (magnetic) input, is the most critical factor in device applications based on these composites.^{1–4} In terms of energy efficiency, it is most desirable that the ME effect be as large as possible. While properly graded composition was shown recently to be capable of enhancing the ME effect,⁵ any imperfect (realistic) interface would reduce the ME effect in terms of the classic composite theory.⁶ Consequently the ferroelectric and ferromagnetic interface, which is responsible for transferring the strains from one phase to another, is critical in achieving a giant ME effect in multiferroic composites. However, recent investigations on the nonideal (or imperfect) interface in multiferroic composites were primarily concerned with the soft interface at which different tangential strains may occur.^{6–9}

Owing to the minimization of components (nanopillars) in nanostructured multiferroic composites,^{10,11} the behavior of interfaces becomes a prominent factor in controlling the magnetoelastoelectric properties and the ME effect of nanostructured multiferroic composites due to the increasing ratio of the interface area to volume. In recent years, therefore, the surface elasticity theory¹² has been developed to account for the effects of surfaces and interfaces at nanoscales.^{13–19} In fact, the surface elasticity theory describes the membrane-type interface, a kind of stiff interface.^{18,20} These studies based on elasticity show that depending upon the interface design, the effective properties of the nanocomposite can be either enhanced or reduced. This size-dependent feature in nanocomposites thus provides an alternative avenue to improve and control material properties in nanocomposites.

Motivated by these exciting works, in this letter, we study the local and overall responses of the multiferroic fibrous nanocomposite by taking into consideration the surface energy along the interface. More specifically, the interface investigated here is mechanically stiff and electromagnetically highly conducting. The magnetoelastoelectric fields in a two-phase composite system composed of a matrix and an isolated circular fiber are derived by ignoring the interactions

between neighboring fibers. Then the effective moduli of the multiferroic nanocomposite with a finite fiber concentration are derived by using the Mori–Tanaka mean-field method.^{21–23} Our numerical results show that the effective stiffness and more importantly the ME effect can be substantially enhanced by properly choosing the interface, providing an opportunity for controlling the ME effect and other effective moduli of the nanocomposites. This result is consistent with a recent observation that nanofiber composites could exhibit a high ME effect.²⁴

Consider an isolated multiferroic fiber with a circular cross section (phase 2) of radius R embedded in an infinite multiferroic matrix (phase 1), as shown in Fig. 1. Both the fiber and matrix have $6mm$ material symmetry about the fiber axis (the z -axis). At infinity, the matrix is subjected to uniform antiplane shear stresses $\sigma_{zx}^\infty, \sigma_{zy}^\infty$, in-plane electric displacements D_x^∞, D_y^∞ and magnetic fluxes B_x^∞, B_y^∞ . Thus the two-phase composite system is in a state of antiplane deformation described by $u_z = w(x, y)$; $\phi = \phi(x, y)$; $\varphi = \varphi(x, y)$, where u_z denotes the nonzero elastic displacement component in z -direction; ϕ and φ are the electric and magnetic potentials.

We now introduce the generalized displacement vector $\mathbf{U} = [w \ \phi \ \varphi]^T$ and generalized stress function vector $\mathbf{\Phi}$, which is related to the stresses, electric displacements, and

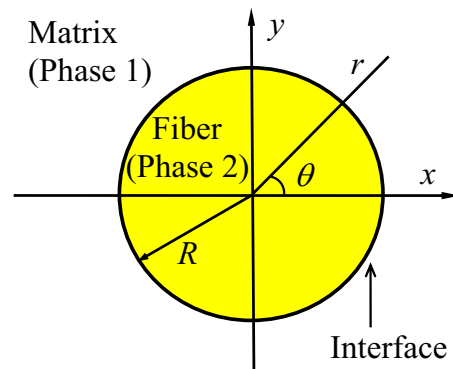


FIG. 1. (Color online) A multiferroic circular cylindrical fiber of radius R bonded to an infinite multiferroic matrix through an interface. The polarization and magnetization directions are along the fiber axis.

^{a)}Electronic mail: pan2@uakron.edu.

magnetic fluxes through the following relations:

$$[\sigma_{zy} \ D_y \ B_y]^T = \Phi_{,x}, \quad [\sigma_{zx} \ D_x \ B_x]^T = -\Phi_{,y}. \quad (1)$$

Then, it can be shown that the generalized displacement and stress function vectors can be concisely expressed in terms of an analytic function vector $\mathbf{f}(z)$ of a single complex variable $z=x+iy=r \exp(i\theta)$ as⁶

$$\mathbf{U} = \text{Im}\{\mathbf{f}(z)\}, \quad \Phi = \mathbf{L} \text{Re}\{\mathbf{f}(z)\}, \quad (2)$$

where

$$\mathbf{L} = \begin{bmatrix} c_{44} & e_{15} & q_{15} \\ e_{15} & -\varepsilon_{11} & -\alpha_{11} \\ q_{15} & -\alpha_{11} & -\mu_{11} \end{bmatrix} \quad (3)$$

is the generalized stiffness matrix, which is real and symmetric but not positive definite.

In nanocomposites, the interfacial stress tensor $\sigma_{\alpha\beta}^s$ is 2×2 symmetric, which is related to the interfacial energy $g(\varepsilon_{\alpha\beta}^s)$ by^{13,18}

$$\sigma_{\alpha\beta}^s = \partial g / \partial \varepsilon_{\alpha\beta}^s + \tau_0 \delta_{\alpha\beta}, \quad (4)$$

where $\varepsilon_{\alpha\beta}^s$ is the 2×2 interfacial strain tensor, $\delta_{\alpha\beta}$ the Kronecker delta, and τ_0 the residual surface tension. If we further assume that the interface is taken as elastically isotropic and that the residual surface tension is ignored, then the interfacial stress tensor can be more specifically expressed as^{18,19}

$$\sigma_{\alpha\beta}^s = 2\mu_s \varepsilon_{\alpha\beta}^s + \lambda_s \varepsilon_{\gamma\gamma}^s \delta_{\alpha\beta}, \quad (5)$$

where μ_s and λ_s are the surface Lamé constants.

For the antiplane shear deformation considered, the elastic continuity conditions on the interface can be expressed as¹⁸

$$w^{(1)} = w^{(2)}, \quad \sigma_{zr}^{(1)} - \sigma_{zr}^{(2)} = -\partial \sigma_{z\theta}^s / (r \partial \theta), \quad (r=R), \quad (6)$$

where the superscripts (1) and (2) denote the associated quantities in the matrix (phase 1) and fiber (phase 2), respectively.

It can be shown that Eq. (6) can be further expressed as

$$w^{(1)} = w^{(2)}, \quad \sigma_{zr}^{(1)} - \sigma_{zr}^{(2)} = -\mu_s \partial^2 w^{(2)} / (r^2 \partial \theta^2), \quad (r=R), \quad (7)$$

which are equivalent to those for a stiff interface. It is noted that μ_s is a nonnegative parameter with $\mu_s=0$ for the perfect elastic interface case, and $\mu_s=+\infty$ for the rigid fiber case. Meanwhile, similar to the highly conducting thermal interface, we assume that the interface is electrically and magnetically highly conducting,²⁵ such that

$$\begin{aligned} \phi^{(1)} &= \phi^{(2)}, \quad D_r^{(1)} - D_r^{(2)} = \delta \partial^2 \phi^{(2)} / (r^2 \partial \theta^2), \\ \varphi^{(1)} &= \varphi^{(2)}, \quad B_r^{(1)} - B_r^{(2)} = \eta \partial^2 \varphi^{(2)} / (r^2 \partial \theta^2), \quad (r=R), \end{aligned} \quad (8)$$

where δ and η are two nonnegative parameters. It is noted that $\delta=\eta=0$ corresponds to an electromagnetically perfect interface, whereas $\delta=\eta=+\infty$ describes an equipotential interface. It is of interest to observe from Eqs. (7) and (8) that boundary conditions for an elastically stiff interface and those for a highly conducting interface are very similar except for a sign difference.

Using the basic formulations presented above, the interface conditions in Eqs. (7) and (8) (at $r=R$) can be concisely expressed in terms of two analytic function vectors, $\mathbf{f}_1(z)$ defined in the matrix and $\mathbf{f}_2(z)$ defined in the fiber as follows:

$$\begin{aligned} \mathbf{f}_2^+(z) - \bar{\mathbf{f}}_2^-\left(\frac{R^2}{z}\right) &= \mathbf{f}_1^+(z) - \bar{\mathbf{f}}_1^-\left(\frac{R^2}{z}\right), \\ \mathbf{L}_1 \mathbf{f}_1^+(z) + \mathbf{L}_1 \bar{\mathbf{f}}_1^-\left(\frac{R^2}{z}\right) - \mathbf{L}_2 \mathbf{f}_2^+(z) - \mathbf{L}_2 \bar{\mathbf{f}}_2^-\left(\frac{R^2}{z}\right) \\ &= \Lambda \left[z \mathbf{f}_2^+(z) + \frac{R^2}{z} \bar{\mathbf{f}}_2^-\left(\frac{R^2}{z}\right) \right], \quad (|z|=R), \end{aligned} \quad (9)$$

where

$$\Lambda(R) = \text{diag}[\mu_s, -\delta, -\eta]/R \quad (10)$$

depends not only on the interface property, but also on the radius of the fiber. Based on the complex analytic function approach,⁶ the two analytic functions can be expressed as

$$\begin{aligned} \mathbf{f}_1(z) &= [\mathbf{I} - 2(\mathbf{L}_1 + \mathbf{L}_2 + \Lambda)^{-1} \mathbf{L}_1] \mathbf{L}_1^{-1} \bar{\mathbf{k}} R^2 z^{-1} \\ &\quad + \mathbf{L}_1^{-1} \mathbf{k} z, \quad (|z| > R), \end{aligned} \quad (11)$$

$$\mathbf{f}_2(z) = 2(\mathbf{L}_1 + \mathbf{L}_2 + \Lambda)^{-1} \mathbf{k} z, \quad (|z| < R), \quad (12)$$

where the vector \mathbf{k} is related to the remote uniform loading as

$$\mathbf{k}^T = [\sigma_{zy}^\infty + i\sigma_{zx}^\infty, D_y^\infty + iD_x^\infty, B_y^\infty + iB_x^\infty]. \quad (13)$$

With these two analytic functions, other field distributions can be subsequently obtained. For example, it is found that the strains, electric, and magnetic fields are all *uniform* but *size-dependent* (due to the appearance of the radius R in Λ) inside the circular fiber. We now assume that the aligned circular cylindrical multiferroic fibers of the same radius are randomly distributed on the x - y plane. By employing the Mori-Tanaka mean field method,²¹⁻²³ the effective moduli of the multiferroic fibrous nanocomposite with interface effects can be finally derived as

$$\begin{aligned} \mathbf{L}_c &= \mathbf{L}_1 [(1+c_2)\mathbf{L}_1 + (1-c_2)(\mathbf{L}_2 + \Lambda)]^{-1} [(1-c_2)\mathbf{L}_1 \\ &\quad + (1+c_2)(\mathbf{L}_2 + \Lambda)], \end{aligned} \quad (14)$$

where c_2 is the volume fraction of the multiferroic fibers. It is important that, since Λ contains the radius of the fibers, the effective moduli of the nanocomposite is size-dependent,²⁶ a phenomenon different from the classical size-independent result.²⁷

We point out that our closed-form solution for the effective moduli (14) contains various previous results as special cases. For instance, when both the fiber and matrix are purely elastic, \mathbf{L}_1 and \mathbf{L}_2 become diagonal; then the effective elastic constant $c_{44}^{(c)}$ of the composite is reduced to the result¹⁸ based on the concept of neutral inhomogeneities. On the other hand when the interface effect is ignored by setting $\Lambda=0$, Eq. (14) is reduced to that for the perfect interface case.²⁷

We further observe from Eq. (14) that the effective moduli of the nanocomposite with interface effects are equivalent to those of a virtual composite where the circular fibers with the *virtual moduli* $\hat{\mathbf{L}}_2 = \mathbf{L}_2 + \Lambda(R)$ are perfectly bonded to the matrix. Therefore, we conclude that incorporation of the interface effect is equivalent to an increase in the values of the stiffness, dielectric permittivity and magnetic permeability of the fibers via the size-dependent interface matrix $\Lambda(R)$.

As a numerical example, we consider the nanostructured BaTiO₃/CoFe₂O₄ multiferroic composite: the piezoelectric

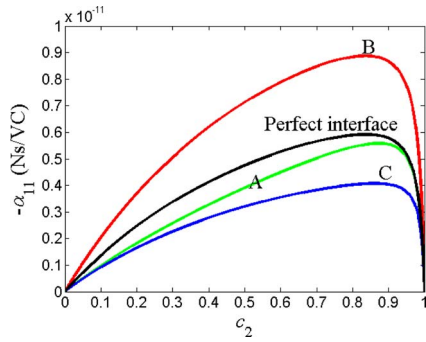


FIG. 2. (Color online) The ME coefficient α_{11} as a function of the CoFe_2O_4 volume fraction c_2 for four different interfaces: Perfect interface ($\mu_s = \delta = \eta = 0$), interface A ($\mu_s = R\epsilon_{44}^{(2)}$, $\delta = \eta = 0$), interface B ($\delta = \frac{1}{2}R\epsilon_{11}^{(2)}$, $\mu_s = \eta = 0$), and interface C ($\eta = \frac{1}{2}R\mu_{11}^{(2)}$, $\mu_s = \delta = 0$). BaTiO_3 matrix reinforced by CoFe_2O_4 fibers.

BaTiO_3 matrix reinforced by the magnetostrictive CoFe_2O_4 nanopillars.^{10,11} Figure 2 shows the ME coefficient α_{11} as a function of the CoFe_2O_4 volume fraction c_2 for four different interfaces: perfect interface ($\mu_s = \delta = \eta = 0$), interface A ($\mu_s = R\epsilon_{44}^{(2)}$, $\delta = \eta = 0$), interface B ($\delta = \frac{1}{2}R\epsilon_{11}^{(2)}$, $\mu_s = \eta = 0$), and interface C ($\eta = \frac{1}{2}R\mu_{11}^{(2)}$, $\mu_s = \delta = 0$). Interface A represents a mechanically stiff interface,²⁶ B an electrically highly conducting interface, and C a magnetically highly conducting interface.^{19,26} It is observed from Fig. 2 that the ME coefficient for both interfaces A and C is reduced as compared to that for a perfect interface; however, the ME coefficient for interface B is substantially enhanced as compared to that for a perfect interface.

Figure 3 plots the ME effect for interface B (i.e., for the electrically highly conducting interface) as a function of the interface parameter $\delta/R\epsilon_{11}^{(2)}$ and volume fraction c_2 . It is interesting that when $\delta/R\epsilon_{11}^{(2)}$ changes from 0 to 1, the maximum magnitude of ME effect achieved at $c_2 = 0.85$ is doubled (6×10^{-12} versus 12×10^{-12}). Most importantly, if we could design the interface to increase $\delta/R\epsilon_{11}^{(2)}$ to, for example, ten, then the ME effect will be roughly increased ten times as compared to the classic composite results. This thus provides an excellent opportunity for enhancing the ME effect in nanocomposites using the unique size-dependent feature. This result is consistent with a recent observation where it was demonstrated that nanofiber composites could exhibit a high ME effect.²⁴

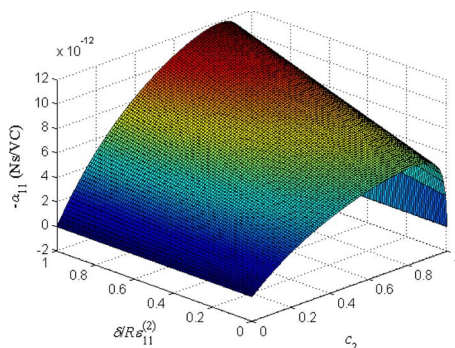


FIG. 3. (Color online) Contour of the ME coefficient α_{11} as a function of the CoFe_2O_4 volume fraction c_2 and interface imperfection $\delta/R\epsilon_{11}^{(2)}$ ($\mu_s = \eta = 0$). BaTiO_3 matrix reinforced by CoFe_2O_4 fibers.

Our results are for a multiferroic nanocomposite consisting of magnetostrictive fibers reinforced in a piezoelectric matrix. For a multiferroic nanocomposite consisting of piezoelectric fibers reinforced in a magnetostrictive matrix, the opposite conclusion can be drawn. In other words, for this case, a magnetically highly conducting interface ($\eta > 0$, $\mu_s = \delta = 0$) can be designed to enhance the ME coefficient.

In conclusion, we show that the nonclassical interface condition exerts a significant influence on the local and overall magnetoelastoelectric responses of the multiferroic composite especially when the fibers are at the nanoscale. We further demonstrate that it is possible to enhance the ME coefficient of a multiferroic composite consisting of magnetostrictive fibers reinforced in a piezoelectric matrix by designing an electrically highly conducting interface.²⁶ Therefore, the present analysis on multiferroic nanocomposites with interface effects²⁸ will provide an alternative opportunity for enhancing the ME effect.

This work was supported in part by AFOSR under Grant No. FA9550-06-1-0317.

- ¹G. Harshé, Ph.D. thesis, Pennsylvania State University, 1991; G. Harshé, J. P. Dougherty, and R. E. Newnham, *Int. J. Appl. Electromagn. Mater.* **4**, 145 (1993); M. Avellaneda and G. Harshé, *J. Intell. Mater. Syst. Struct.* **5**, 501 (1994).
- ²M. Fiebig, *J. Phys. D: Appl. Phys.* **38**, R123 (2005).
- ³W. Eerenstein, N. D. Mathur, and J. F. Scott, *Nature (London)* **442**, 759 (2006).
- ⁴C. W. Nan, M. I. Bichurin, S. X. Dong, D. Viehland, and G. Srinivasan, *J. Appl. Phys.* **103**, 031101 (2008).
- ⁵X. Wang, E. Pan, J. D. Albrecht, and W. J. Feng, *Compos. Struct.* **87**, 206 (2009); V. M. Petrov and G. Srinivasan, *Phys. Rev. B* **78**, 184421 (2008).
- ⁶X. Wang and E. Pan, *Phys. Rev. B* **76**, 214107 (2007).
- ⁷C. W. Nan, G. Liu, and Y. H. Lin, *Appl. Phys. Lett.* **83**, 4366 (2003).
- ⁸M. I. Bichurin, V. M. Petrov, and G. Srinivasan, *Phys. Rev. B* **68**, 054402 (2003).
- ⁹C. M. Chang and G. P. Carman, *Phys. Rev. B* **76**, 134116 (2007).
- ¹⁰H. Zheng, J. Wang, S. E. Lofland, Z. Ma, L. Mohaddes-Ardabili, T. Zhao, L. Salamanca-Riba, S. R. Shinde, S. B. Ogale, F. Bai, D. Viehland, Y. Jia, D. G. Schlom, M. Wuttig, A. Roytburd, and R. Ramesh, *Science* **303**, 661 (2004).
- ¹¹C. W. Nan, G. Liu, and Y. H. Lin, *Phys. Rev. Lett.* **94**, 197203 (2005).
- ¹²R. C. Cammarata and K. Sieradzki, *Annu. Rev. Mater. Sci.* **24**, 215 (1994).
- ¹³W. D. Nix and H. Gao, *Scr. Mater.* **39**, 1653 (1998).
- ¹⁴P. Sharma, S. Ganti, and N. Bhate, *Appl. Phys. Lett.* **82**, 535 (2003).
- ¹⁵F. Q. Yang, *J. Appl. Phys.* **95**, 3516 (2004); **99**, 054306 (2006).
- ¹⁶H. L. Duan, J. Wang, Z. P. Huang, and B. L. Karihaloo, *J. Mech. Phys. Solids* **53**, 1574 (2005).
- ¹⁷G. F. Wang, T. J. Wang, and X. Q. Feng, *Appl. Phys. Lett.* **89**, 231923 (2006).
- ¹⁸T. Chen, G. J. Dvorak, and C. C. Yu, *Acta Mech.* **188**, 39 (2007).
- ¹⁹V. B. Shenoy, *Phys. Rev. B* **71**, 094104 (2005); S. Pathak and V. B. Shenoy, *ibid.* **72**, 113404 (2005).
- ²⁰Y. Benveniste and T. Miloh, *Mech. Mater.* **33**, 309 (2001).
- ²¹T. Mori and K. Tanaka, *Acta Metall.* **21**, 571 (1973).
- ²²G. J. Weng, *Int. J. Eng. Sci.* **22**, 845 (1984).
- ²³T. Chen, G. J. Dvorak, and Y. Benveniste, *ASME J. Appl. Mech.* **59**, 539 (1992).
- ²⁴C. L. Zhang, W. Q. Chen, S. H. Xie, J. S. Yang, and J. Y. Li, *Appl. Phys. Lett.* **94**, 102907 (2009).
- ²⁵T. Chen, *Int. J. Solids Struct.* **38**, 3081 (2001).
- ²⁶T. Chen and G. J. Dvorak, *Appl. Phys. Lett.* **88**, 211912 (2006); T. Chen, M. S. Chiu, and C. N. Weng, *J. Appl. Phys.* **100**, 074308 (2006).
- ²⁷Y. Benveniste, *Phys. Rev. B* **51**, 16424 (1995).
- ²⁸B. M. Clemens, W. D. Nix, and V. Ramaswamy, *J. Appl. Phys.* **87**, 2816 (2000); C. G. Duan, S. S. Jaswal, and E. Y. Tsymlal, *Phys. Rev. Lett.* **97**, 047201 (2006).